Solid-State Characterization and Role of Solvent Molecules on the Crystal Structure, Packing and Physiochemical Properties of Different Quercetin Solvates

Panayiotis Klitou[1], Christopher M. Pask[2], Larisa Onoufriadi[3], Ian Rosbottom[4], Elena Simone[1]*

[1]School of Food Science and Nutrition, Food Colloids and Bioprocessing Group, University of Leeds, Leeds, UK

[2] School of Chemistry, University of Leeds, Leeds, UK

[3] School of Chemical and Process Engineering, University of Leeds, Leeds, UK

[4] Department of Chemical Engineering, Imperial College London, South Kensington Campus, London, UK

*Corresponding author: e.simone@leeds.ac.uk

Keywords: quercetin, solvates, synthonic modelling

ABSTRACT

In this work a novel quercetin and dimethyl sulfoxide (DMSO) solvate (QDMSO) crystal structure was grown from a mixture of DMSO and water as solvent. Quercetin is a naturally occurring bioflavonoid widely used in the nutraceutical industry due to its many health benefits. Understanding quercetin solvates formation is essential for the design of novel particulate products with tailored quality attributes, including solubility, thermal resistance and bioavailability.

Here, the physiochemical properties and phase transitions of QDMSO were characterized by a wide range of experimental techniques, and the crystal structure, molecular packing and intermolecular interactions (synthons) within the crystal lattice were modelled. Modelling and experimental results were compared to those of other known quercetin crystal structures, an anhydrous, a monohydrate and a dihydrate form, to elucidate the role of the solvent molecules on the molecular packing and intermolecular interactions and, ultimately, on the physiochemical properties of each crystal form. It was found that in QDMSO, hydrogen bonds and dipole-dipole interactions had a greater contribution to the total lattice energy, and quercetin-solvent hydrogen bonds were stronger in energy compared to those of the other quercetin structures. These findings were used to explain the superior thermal stability of the QDMSO structure as well as its moisture-dependent behavior. This work demonstrates a coupled modelling and experimental methodology that relates intermolecular interactions and molecular packing in different solvated forms to physiochemical properties and can help in a better prediction and design of particulate products via rational choice of the solid form.

INTRODUCTION

Solvates and hydrates are multicomponent crystalline solids that comprise a host molecule and a guest solvent molecule in the crystal lattice.[1] Many active pharmaceutical ingredients (APIs) and food grade substances can form these structures.[1],[2] The presence of guest solvent molecules within the crystal can affect the molecular conformation of the host molecule within the structure, as well as the type and strength of intermolecular interactions that characterize the crystal lattice, resulting in different physiochemical properties, such as thermodynamic stability, solubility, dissolution rate and bioavailability. [3],[4],[5],[6]

Hydrate/solvate formation can then be exploited to safely manipulate the physiochemical properties of crystals in order to achieve desired quality attributes such as improved solubility and bioavailability.[7] In fact, many pharmaceutical products are marketed as solvated crystal forms, for example amoxicillin trihydrate and darunavir ethanolate.[8],[9] De-solvation of a solvated crystal form can also provide an alternative pathway to the formation of polymorphic forms that would otherwise be difficult or impossible to crystallize by conventional crystallization techniques.[6] These are typical examples of crystal engineering approaches, which focuses on controlling the way that molecules crystallize to produce materials and final products with tailored properties.[10]

In some cases, unexpected transformations of the unsolvated crystals to their solvated forms, or even between different solvated forms, can happen during manufacturing or storage,[11],[12] These transformations can cause undesired physiochemical properties of the final marketed products, compromising their quality and thus incurring extra costs and safety risks for the consumers. [11],[6] It is, therefore, imperative to know how crystallization parameters, for example choice of solvent, or environmental conditions during storage, like temperature and relative

humidity, could induce any phase transitions between the different crystal forms of a crystalline material.[13]

Quercetin, 2-(3,4-Dihydroxyphenyl)-3,5,7-trihydroxy-4H-chromen-4-one, is a naturally occurring flavonoid found in many fruits and vegetables (e.g., onions, berries and tomatoes) as well as in tea, wine and vinegar. [14],[15] Quercetin has recently stimulated considerable interest within the nutrition and food science communities due to its significant association between dietary consumption and various health benefits, including antioxidant, anti-inflammatory and antitumor activities. [16],[15],[14],[17] Due to this vast range of biological effects, quercetin finds use in the nutraceutical industry and as a food supplement product. [15]

Quercetin has been reported to exist as anhydrous, monohydrate and dihydrate crystal forms. [18],[19],[14],[20],[21] A previous study identified how water molecules in the hydrated structures of quercetin could impact significantly upon packing and conformation energetics of these forms, as compared to the anhydrous form.[22] Quercetin dihydrate, the commercial form of this compound, has been studied experimentally using a wide range techniques, and has been identified as the most thermodynamically stable form at ambient conditions. [23],[24] However, there has been relatively little work to explore other possible solvated forms of quercetin, which could have superior physical properties for formulation in food products.

In this work, we further explored the solid-state landscape of quercetin by crystallizing this molecule in mixtures of dimethyl sulfoxide (DMSO) and water. Quercetin is characterized by a very low water solubility, which results in difficulties in growing quercetin crystals from water. [15] Therefore, mixtures of DMSO and water were used to improve yield of crystallization as well as to achieve larger crystals, since DMSO has the ability to solubilize a wide range of otherwise insoluble or sparingly soluble substances.[25]

A novel crystal structure of quercetin, a quercetin-DMSO solvate (QDMSO), was discovered and comprehensively characterized by a range of analytical techniques. This was underpinned by molecular modelling of the molecular conformation and packing energetics to discover the role of the DMSO solvent molecule. The modelling work was compared to that of other quercetin structures – quercetin dihydrate (QDH), quercetin monohydrate (QMH), and quercetin anhydrous (QA), to evaluate the effect of the solvent molecules on the type and strength of intermolecular interactions, conformation and packing arrangements in the crystals. This information was then related to the physiochemical properties of these structures, for example the thermal and moisture-dependent stabilities.[22],[24] This proposed working framework for the analysis of solvated structures can be extremely valuable when designing products, processes and storage conditions for particulate products with known solvated forms.[26],[27]

EXPERIMENTAL SECTION

Materials. Quercetin dihydrate with a purity of 97% w/w was obtained from Alfa Aesar (Port of Heysham Industrial Park, Lancashire, England) while dimethyl sulfoxide (DMSO) solvent was purchased from Fisher Scientific (Bishop Meadow Road, Loughborough, England). Water purified by treatment with a Milli-Q apparatus was used. Quercetin dihydrate was used as received for the solid-state characterization.

Preparation of Quercetin-DMSO solvate (QDMSO). QDMSO was obtained by preparing several 70g solutions of different DMSO/water ratios, ranging from 50%(w/w) to 80%(w/w) DMSO. Each solution was made to be saturated at around 55°C by continuously dissolving quercetin dihydrate crystals at such temperature, until further dissolution was not possible. The temperature of the solutions was then reduced to 15 °C at a cooling rate of -0.1 °C/min. This

procedure allowed obtaining plate-like crystals of QDMSO, of sizes ranging from 50µm to 300µm depending on the conditions of crystallization. The temperature of the 70%(w/w) DMSO solution was then cycled from 15 °C to 23 °C at a cooling/heating rate of -0.5 °C/min for three days, to promote growth of the crystals to a final size of approximately 500µm, which was suitable for single crystal X-ray diffraction (SCXRD). The temperature was controlled using a Huber Ministat 230 thermoregulator connected to a 100mL jacketed vessel. The crystals were then filtered using filter paper and dried without any further washing.

Single Crystal X-ray Diffraction (SCXRD). Measurements were carried out at 120K on an Agilent SuperNova diffractometer equipped with an Atlas CCD detector and connected to an Oxford Cryostream low temperature device using mirror monochromated Cu Kα radiation (λ = 1.54184 Å) from a Microfocus X-ray source. Crystals of dimensions 0.55 × 0.36 × 0.06 mm^3 were used. The structure was solved by intrinsic phasing using SHELXT and refined by a full matrix least squares technique based on F2, using SHELXL2014.[28,29] All non-hydrogen atoms were located in the Fourier Map and refined anisotropically. All carbon-bound hydrogen atoms were placed in calculated positions and refined isotropically using a "riding model". All oxygen-bound hydrogen atoms were located in the Fourier Map and refined isotropically. The structure exhibited disorder where one molecule of DMSO was modelled across two positions in an 85:15 ratio. For the purposes of the computational studies shown in this work the minor component was disregarded and a modified cif file was generated that only modelled the 85% position of the DMSO molecule. For the new QDMSO structure found the crystallographic .cif file (CCDC No. 1971580) is available free of charge at https://www.ccdc.cam.ac.uk/structures/.

Variable Temperature Powder X-ray Diffraction (VT-PXRD). PXRD patterns were collected on a Panalytical X'Pert PRO, which was set up in Bragg -Brentano mode, using Cu

Kα radiation (λ = 1.54184 Å), in a scan between 5° to 90° in 2θ with a step size of 0.032° and time per step 25 seconds. Temperature was varied from 25 °C to 180 °C.

Thermogravimetric Analysis coupled with Differential Scanning Calorimetry (TGA/DSC). TGA and DSC experiments were performed on a Mettler Toledo TGA/DSC 3+ Stare System equipment. The samples (around 10-15mg) were placed in 70µl aluminium pans, covered with a lid, and heated from 25 to 600°C at a heating rate of 10 °C.min^{-1}. Nitrogen was used as the purge gas at 50 mL min^{-1}. The measurements were repeated three times for each sample.

Hot Stage Microscopy (HSM). All HSM experiments were performed on a Leitz Dialux 22 Polarized microscope (Leica, Germany) equipped with a controlled heating and cooling stage CSS450 (Linkam, Surrey, UK) controlled by the Linksys 32 software (Linkam, Surrey UK) and an imaging system (Canon EOS 7D Mark II DSLR Camera) at 40X magnifications. The samples were heated over a temperature range of 25−150 °C at a constant heating rate of 10 °C min^{-1}.

Dynamic Vapour Sorption (DVS). Dynamic vapour sorption experiments were performed on a Surface Measurement Systems DVS Resolution equipment. Measurements were carried out over a humidity range of 0%-90% relative humidity (RH) at 25°C. Each humidity step was terminated when less than 0.02% sample weight change was observed or when a maximum hold time of 360 mins was reached. Each measurement was repeated at least twice.

Scanning Electron Microscopy (SEM). The dry samples were imaged using a Carl Zeiss EVO MA15 scanning electron microscope at magnifications from 50X to 200X. Samples were arranged on Leit tabs attached to SEM specimen stubs and an Iridium coating was applied before measurement.

Computational Analysis. As mentioned earlier, for the purposes of computational modelling the modified .cif file of the QDMSO structure that modelled only the 85% position of the DMSO molecule was used. Computational analysis was performed using Materials Studio 2017, HABIT98, and Mercury software. [30,31,32] The crystal structure was minimized using the Forcite module in Materials Studio 2017, using the same methodology described in previous publications. [22,30] The files were exported as .car files (Cartesian coordinates), converted to fractional coordinates, and then fractional charges were calculated using the AM1 method within MOPAC.[33] The bulk intrinsic synthon analysis was carried out using the HABIT98 software, which takes in structural information to construct a series of unit cells in three dimensions, and calculates the pairwise intermolecular interaction between a molecule in the origin unit cell and all the other molecules within a fixed radius of 30Å from the central molecule. [31,34,35] The calculation of intermolecular interaction energies was performed using the Dreiding II force-field.[36] The ranking of the intermolecular interactions by strength was outputted using the DEBUG-1 function. All visualization of molecular and crystal packing were carried out in Mercury CSD 3.10.[32]

RESULTS

Quercetin-DMSO solvate (QDMSO) Single Crystal Structure. Cooling of all the saturated solutions of quercetin in the DMSO-Water mixture solvents (from 50% to 80% w/w DMSO) resulted in the formation of colorless plate-like crystals. However, crystals of suitable size for SCXRD were only obtained from the 70%(w/w) DMSO solution at the end of the temperature cycling period. The crystal structure was identified as a quercetin-DMSO solvate that crystallized in a monoclinic cell. SEM images of the crystals are shown in Figure 1, QDMSO present a plate-like morphology. The structure was solved in the *I*2/*a* space group, with two

molecules of quercetin and three molecules of DMSO in the asymmetric unit. The structure exhibited disorder, where one of the three DMSO molecules was modelled across two positions in an 85:15 ratio. The crystallographic data and structure refinement data for the QDMSO structure are presented in Supporting Information Table S1.

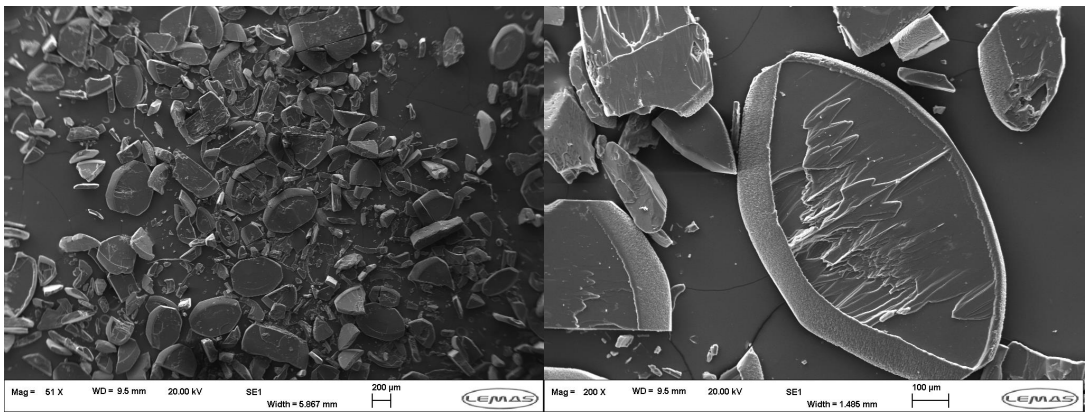

Figure 1. SEM images of QDMSO at 51X (left) and 200X (right) magnification.

The PXRD pattern obtained experimentally from the bulk powder samples and the simulated one from the cif file in Mercury (calculated based on the QDMSO single crystal structure solved) are shown in Figure 2. The two patterns closely matched confirming that the bulk sample is a highly pure phase and the single crystal is representative of the bulk material. A slight shift in the whole pattern was observed between the experimental and simulated patterns due to the fact that the SCXRD was run at 120K while the PXRD was performed at room temperature (25 °C). The higher temperature at which the PXRD was run resulted in a general expansion of the unit cell of the structure, resulting in the observed shift in the pattern.

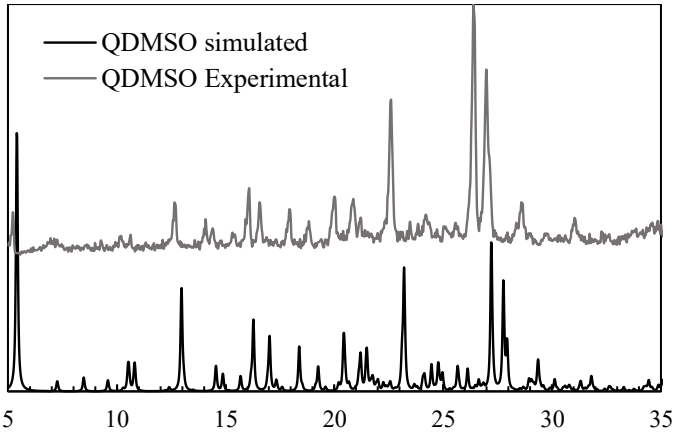

Figure 2. PXRD pattern for QDMSO obtained experimentally and simulated from crystal structure.

The DMSO solvate crystallizes with two quercetin molecules (Q1 & Q2) and three DMSO molecules (D1, D2 & D3) in the asymmetric unit (Figure 3a). This arrangement allows all of the carbonyl and hydroxyl groups to form at least one intermolecular hydrogen bond, whereby several of the hydroxyl groups act as both H-bond acceptors and donors. This creates 'cooperative hydrogen bonds', whereby all the hydrogen bonds formed from these groups will be strengthened.[37]

Figure 3 shows that the H-bonding provided by the DMSO molecules allows the unbroken chain of close stacking of the quercetin molecules along the b-axis (Figure 3c). These interactions have previously been shown to be important in stabilizing the hydrated structures of quercetin.[22] Most of the hydrogen bonds are aligned in the OC/OA plane (Figure 3b), since the stacking of the quercetin molecules along the b-axis requires a planar conformation of the quercetin molecules, which in turn arranges the H-bonds to be planar as well. Though there is a limited amount of H-bonding shown in Figure 3d, due to the DMSO molecules filling spaces in the direction of the a-axis, the H-bonds are not all aligned specifically in one direction, forming unbroken chains instead.

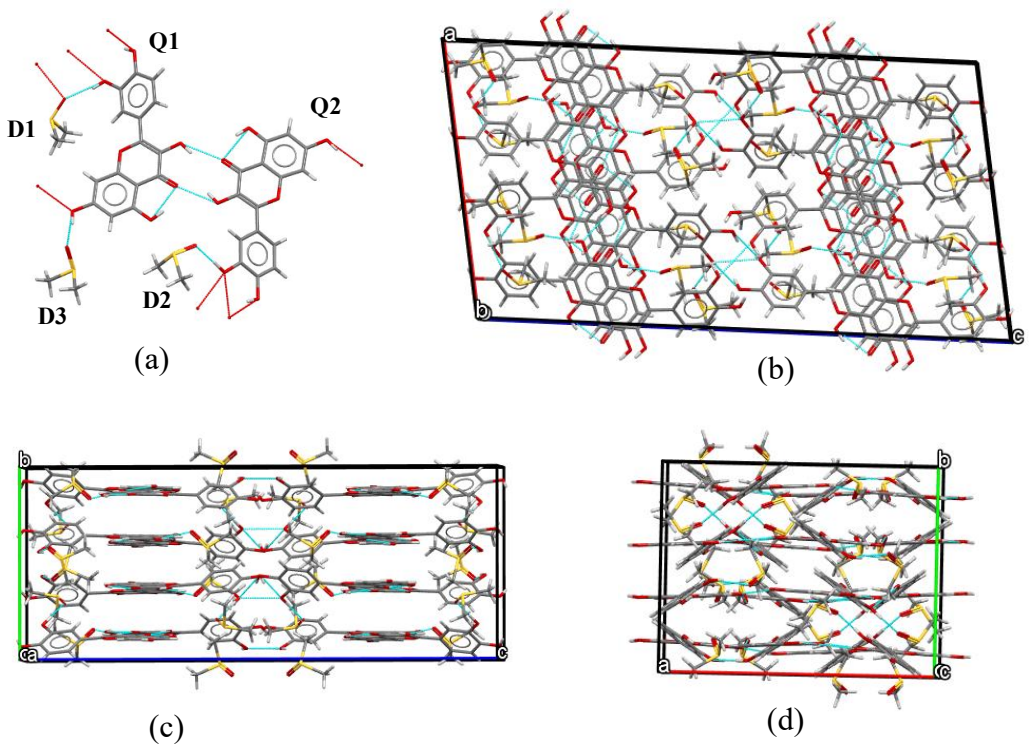

Figure 3. The packing diagrams for the QDMSO solvate structure. (a) The asymmetric unit with the H-bonds to neighboring molecules shown as 'hanging'; (b) the OC/OA view of the unit cell, where the majority of H-bonds are formed; (c) the OB/OC view of the unit cell showing the close stacking of the quercetin molecules; (d) the OA/OB view of the unit cell showing a limited amount of H-bonding in this direction.

The arrangement of the DMSO molecules shows that they are woven tightly into the arrangement of the quercetin molecules, without any obvious channel for de-solvation. The strong synergistic H-bonding and lack of an obvious de-solvation route may be reason for the superior thermal stability of the DMSO solvate.

When considering the arrangement of this solvate, as compared to the hydrated and non-solvated forms, it seems that the increasing presence of solvent encourages the planar close packing of the quercetin molecules.[22] Indeed, as the solvent/solute ratio increases, the propensity for all the quercetin molecules to align and stack in one direction increases. Such

packing characteristics have been linked with crystal forms that are relatively easy to nucleate and grow, in particular showing needle like morphologies.[38,39]

The torsion angle of the pyrone to the phenyl ring for both molecules in the asymmetric unit of QDMSO was measured: τ1 represents the torsion angle for molecule Q1 while τ2 is the torsion angle for Q2. It was found that τ1 and τ2 for the two quercetin molecules of the asymmetric unit have slightly different torsion angles of 30.71° and 31.11°, respectively, as shown in Figure 4.

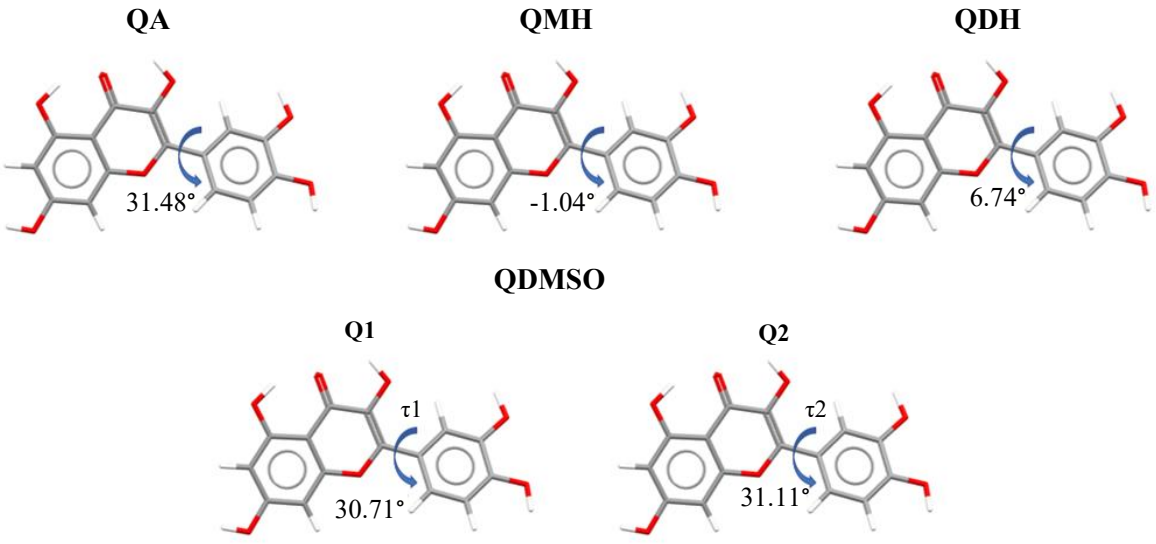

Figure 4. Torsion angles of phenyl to pyrone rings for quercetin molecules in quercetin structures (quercetin anhydrous – QA, quercetin monohydrate – QMH, quercetin dihydrate – QDH, quercetin – DMSO solvate – QDMSO). [22]

A previous study identified that the quercetin molecules in the QMH and QDH structures were close to planar, as the water molecules helped in satisfying the hydrogen bonding sites on the quercetin molecule, and the planar conformation facilitated close packing and favourable quercetin-quercetin stacking interactions.[22] In comparison, the quercetin conformation in the QA structure was found to be almost identical to that found in the new QDMSO structure.

Since DMSO only has no hydrogen bonding hydrogens and only one hydrogen bonding oxygen, in combination with it being bulkier than water, results in it being far less effective at hydrogen bonding. Hence, the quercetin molecule must adopt the twisted conformation to maximise its quercetin-quercetin hydrogen bonds.

Bulk Synthon Analysis for QDMSO. The six strongest intermolecular interactions in the QDMSO structure are illustrated in Figure 5, in order of strength. For each synthon the packing of molecules in the lattice is presented and a closer view on the two interacting molecules for each synthon is also included. The properties of each studied synthon are summarised in Table 1. The first two strongest interactions, QDMSO1 and QDMSO2, are both π-π stacking interactions contributing to growth along the b-axis of the unit cell. In QDMSO1 the phenyl rings of the interacting molecules face opposite directions, while in QDMSO2 these rings face the same direction. The centroid-centroid distances of the quercetin molecules in the two interactions are similar (5.998Å in QDMSO1 and 5.034Å in QDMSO2). However, the interplanar angles differ significantly. In QDMSO1 the interplanar angle is 3.64° while in QDMSO2 it is 22.73°, meaning that QDMSO2 does not result in a parallel packing of the quercetin molecules in the lattice as much as QDMSO1 does. Table 1 shows that for both interactions the contributions of the aromatic rings (pyrone and phenyl) to the total energy of each synthons are high, about 55.8% and 74.4% for QDMSO1 and QDMSO2 respectively. Instead, the contribution from the hydroxyl groups are lower, meaning that QDMSO1 and QDMSO2 are mostly non-polar synthons. The 5th strongest interaction, QDMSO5, is another non-polar interaction due to the high contribution of the aromatic rings. The quercetin molecules pack in a parallel orientation (interplanar angle is 0.00°). However, the offset between the molecules is much greater, having a centroid-centroid distance of 9.995Å. The multiplicity of this interaction is 1 since only one of the two quercetin molecules of the asymmetric unit forms this interaction. This means that this specific interaction is encountered

half the times compared to others that have a multiplicity of 2; this reflects on the contribution of the specific interaction on the total lattice energy.

The 3rd and 4th strongest interactions, QDMSO3 and QDMSO4, are double hydrogen bonding interactions between a hydroxyl and a carbonyl group (for QDMSO3) and two hydroxyl groups (for QDMSO4) of two adjacent quercetin molecules. For QDMSO3 it was found that the contribution of hydroxyl groups (34.5%) and carbonyl groups (11.1%) to the total synthon energy are relatively high, which indicates that this interaction is mostly polar. For QDMSO4, the contribution of hydroxyl groups to the synthon energy is very high, 83.1%, marking this interaction as the most polar of the key synthons presented here.

The quercetin molecules in the QDMSO structure are found to form hydrogen bonds with the DMSO molecules. QDMSO6, is a hydrogen bond between a hydroxyl hydrogen on the phenyl ring of a quercetin molecule and a sulfinyl oxygen of a DMSO molecule. QDMSO6, which is the strongest quercetin-DMSO hydrogen bond in QDMSO, is found to be much higher in energy, -4.14 kcal.mol^{-1}, compared to the strongest quercetin-solvent interaction in QMH (QMH3=-2.55 kcal.mol^{-1}) or QDH (QDH2=-1.71 kcal.mol^{-1}) suggesting that quercetin-DMSO hydrogen bonds are stronger in energy compared to quercetin-water interactions.

A closer look at the hydrogen bonding network in the structure reveals that the first quercetin molecule of the asymmetric unit, Q1, forms 6 hydrogen bonds, of which 3 are with 3 DMSO molecules and 3 with 2 quercetin molecules. The second quercetin molecule of the asymmetric unit, Q2, forms 6 hydrogen bonds, of which 1 is with a DMSO molecule and 5 are with 3 other quercetin molecules. This information is summarised on Table S2 in Supporting Information.

QDMSO1

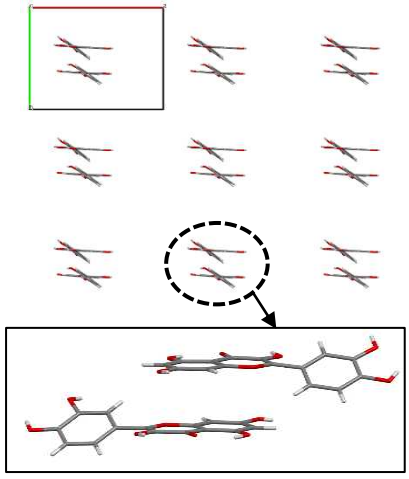

QDMSO2

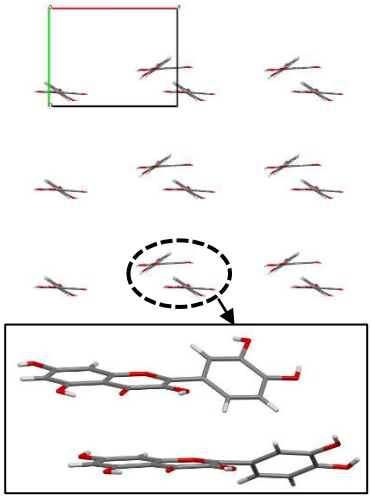

QDMSO3

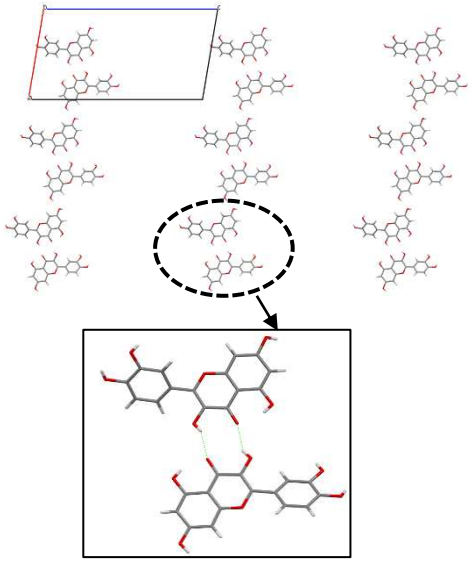

QDMSO4

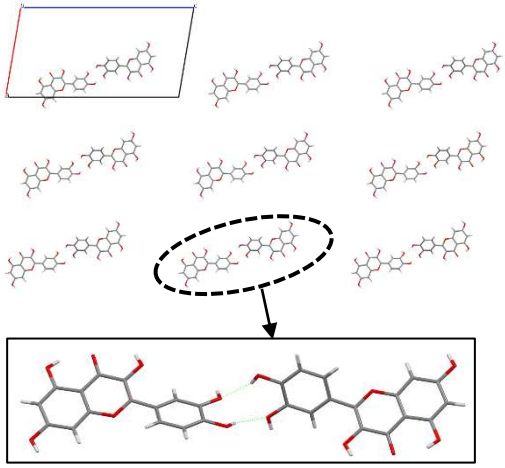

QDMSO5

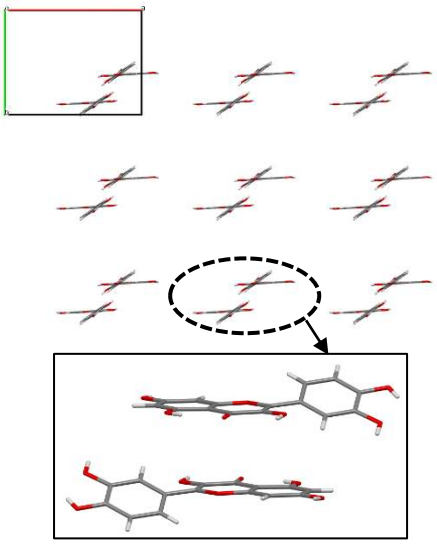

QDMSO6

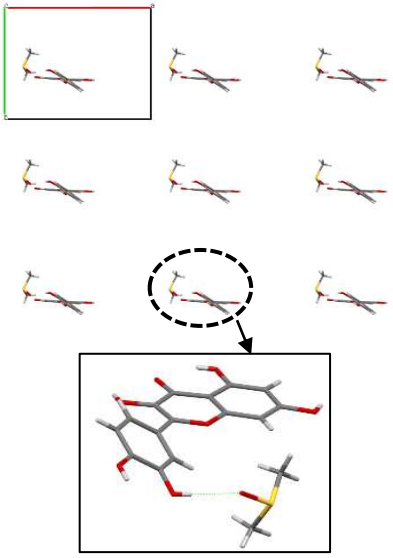

Figure 5. Main bulk intrinsic synthons in QDMSO ordered by strength (green dotted lines indicate hydrogen bond).

Table 1. Summary of bulk intrinsic synthons in QDMSO.

Synthon name	QDMSO1	QDMSO2	QDMSO3	QDMSO4	QDMSO5	QDMSO6
Molecules involved	Q-Q	Q-Q	Q-Q	Q-Q	Q-Q	Q-D
Synthon type	π-π stacking	π-π stacking	H-bond	H-bond	π-π stacking	H-bond
Intermolecular distance (Å)	5.83	5.05	8.36	13.12	6.69	5.27
Synthon energy ($kcal.mol^{-1}$)	-7.37	-5.74	-5.42	-4.87	-4.24	-4.14
Multiplicity	2	2	2	1	1	2
% contribution of synthon to total lattice energy	6.2%	4.8%	4.5%	2.1%	1.8%	3.5%
% contribution of aromatic rings to synthon	55.8%	74.4%	54.4%	21.3%	63.6%	33.3%
% contribution of hydroxyl groups to synthon	22.2%	15.2%	34.5%	83.1%	34.3%	45.2%
% contribution of carbonyl bond to synthon	22.0%	10.4%	11.1%	-4.4%	2.0%	21.5%

Comparison of quercetin structures. A comparison of the modelling work for the different quercetin structures (QDMSO, QDH, QMH and QA) has been conducted and the main findings are summarised in Table 2. A more extensive comparison can be found in Supporting Information Table S3.[22] As discussed earlier, the asymmetric units of the quercetin structures contain: two molecules of quercetin and three molecules of DMSO in QDMSO, one molecule of quercetin and two molecules of water in QDH, one molecule of quercetin and one molecule of water in QMH and one molecule of quercetin in QA. It was found that the unit cell densities

for the solvated structures were very similar and higher than that of QA (0.964 u/Å^3 and 1.007 u/Å^3 for QDH and QMH respectively, while 0.702 u/Å^3 for QA), due to the formation of hydrogen bonds with the solvent molecules that result in a more close-packed structure. The unit cell density of QDMSO was found to be slightly lower than those of QMH and QDH, possibly because of the less planar conformation of the quercetin molecule in QDMSO.

The contribution of the quercetin-solvent interactions to the lattice energy was found to be very high for QDMSO (45.1%) and QDH (45.9%) and considerably lower for QMH (27.2%). This emphasizes that both QDMSO and QDH are structures where the quercetin-solvent interactions are critical for the stabilization of the lattice. The loss of those interactions, due to a heat-induced de-solvation for example, could result in a thermodynamically unstable structure. It should be noticed that although the first five strongest synthons for QDMSO are quercetin-quercetin interactions, QDMSO6 and many the following synthons are quercetin-DMSO interactions.

Table 2. Comparison of quercetin structures.[22]

	QDMSO	QDH	QMH	QA
Unit cell Density (u/Å^3)	0.900	0.964	1.007	0.702
Interactions' contribution to lattice energy:*				
Quercetin – Quercetin	45.1%	53.8%	72.6%	100%
Quercetin – Solvent	45.1%	45.9%	27.2%	-
Solvent – Solvent	9.7%	0.3%	0.2%	-
Contribution of Van der Waals interactions to lattice energy*	60.8%	91.2%	89.1%	92.1%
Contribution of hydrogen bonds and dipole-dipole interactions to lattice energy*	39.2%	8.8%	10.9%	7.9%
Q-Q H-bonds (per quercetin molecule)	3 for Q1 5 for Q2	0	6	6
Q-solvent H-bonds (per quercetin molecule)	3 for Q1 1 for Q2	6	4	-

* Based on the energy of interactions

Summing the energies of these quercetin-QDMSO interactions the overall contribution is very high (45.1%) and equal to the overall contribution of all the quercetin-quercetin interactions. Comparing the main bulk synthons, while in QDH and QMH there is only one type of π-π stacking interaction, in QDMSO there are several different π-π stacking interactions (QDMSO1, QDMSO2, QDMSO5).[22] However, in these interactions the quercetin molecules are not found to stack as closely as in QDH or QMH, as seen by comparing the intermolecular distances of QDMSO1 and QDMSO2 to those of QDH1 and QMH1. This is probably due to the less planar conformation of the quercetin molecule in QDMSO compared to QDH and QMH.

The contribution of hydrogen bonds and dipole-dipole interactions to the lattice energy is more significant for QDMSO (39.2%) compared to all the other structures, for which those interactions contribute to less than around 11%. This indicates that quercetin-quercetin and quercetin-DMSO hydrogen bonds and other polar interactions in QDMSO are stronger in energy compared to other quercetin crystal structures. Moreover, in our previous work it was stated that for QA, QMH and QDH, as the number of water molecules in the unit cell increases, hydrogen bonding is more satisfied by interactions with the incorporated water molecules than by quercetin-quercetin interactions.[22] For QDMSO, hydrogen bonding is partially satisfied between quercetin-quercetin and quercetin-DMSO molecules. Although the quercetin-DMSO hydrogen bonds are favourable and relatively higher in energy compared to the quercetin-water hydrogen bonds, the much larger size of the DMSO molecule compared to water does not allow these molecules to be positioned close to all the polar groups of the quercetin molecules to completely satisfy all hydrogen bonds. Thus, hydrogen bonds are also formed and satisfied among quercetin molecules, which attain a less planar conformation to facilitate interaction between their polar groups.

Thermal analysis (DSC-TGA). Experimental characterisation for the quercetin structures was only performed for QDMSO and QDH as it was very difficult to obtain pure forms of QMH and QA, which were stable for long enough to allow any characterization. Furthermore, the pure form of quercetin obtained from the de-solvation of QDMSO and QDH, as discussed below, did not match the deposited PXRD pattern of QA, therefore it could not be related to the modelling work previously performed.

The differential scanning calorimetry coupled with thermogravimetric analysis of QDMSO and QDH was performed to evaluate the thermal stability of the quercetin structures, and results are shown in Figure 6. Two endothermic peaks were observed for QDH, which were identified as the dehydration and melting of the solid. The dehydration peak was accompanied with a weight loss of 10.0%, as shown in the TGA curve. This is very close to the calculated theoretical loss in mass (10.7%) that would result from the loss of two water molecules per molecule of quercetin, confirming the 1:2 stoichiometry of QDH. The onset temperature for dehydration was found to be approximately 95°C, in agreement with previously published data.[24],[40] There was only one endothermic peak related to dehydration of the QDH, meaning that the two water molecules are lost from the crystal lattice in one single dehydration step. The second endotherm, which corresponds to the melting of the dehydrated form, was observed at an onset temperature of 316°C. The melting temperature agrees with previous studies on the thermal stability of quercetin. [24,40] A second loss in mass, corresponding to the decomposition of quercetin was observed at 330°C, together with an exotherm peak in the DSC curve.

Upon heating the QDMSO structure, two weight losses were observed in the TGA data, corresponding to de-solvation and the molecular decomposition. The onset temperature for de-solvation was 136°C, as confirmed by the DSC endotherm at that temperature. The endotherm for de-solvation exhibits a shoulder at around 167°C, and the endset temperature for the de-solvation from the TGA curve was found to be 197°C, which could indicate that the

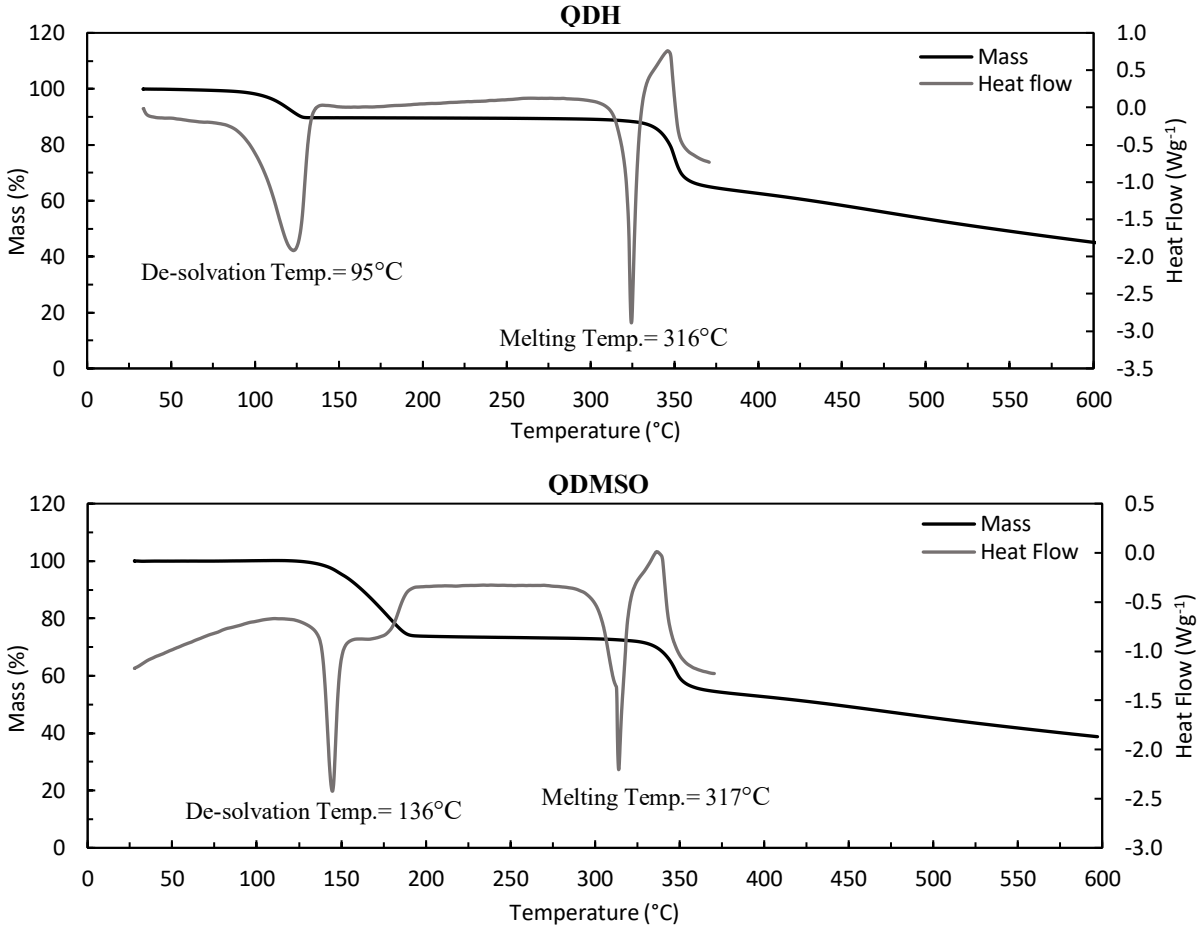

Figure 6. DSC and TGA curves for QDH (top) and QDMSO (bottom).

DMSO molecules are lost from the lattice not in one single de-solvation step but in more consecutive steps. This result was observed in all three repeats of the DSC-TGA analysis performed. The observed loss in mass after complete de-solvation, 26.4%, is close to the theoretical value of 27.9% for a stoichiometry of 1:1.5. The endotherm peak onset temperature for melting was obtained at 317°C. A small shoulder appeared just before the melting peak and it was observed only in one of three measurements carried out on QDMSO. The shoulder could be due to the presence of an impurity in the sample, which probably originated from the purchased quercetin (97% w/w purity). The decomposition takes place at 331°C. All information obtained by DSC-TGA is summarized in Supporting Information Table S4.

Hot Stage Microscopy (HSM). The temperature at which de-solvation of QDMSO was observed using HSM was consistent with the onset de-solvation temperature as calculated by DSC. It was found that the colourless plate-like crystals of QDMSO were transparent at temperatures between 25 °C to 130 °C, after which the crystals appeared to darken and became less transparent due to structural changes related to the loss of solvent. At 140 °C the crystals were completely opaque but maintained the plate-like shape, as shown in Figure 7. The HSM onset temperature (130 °C) agrees with the DSC onset temperature for the loss of the DMSO solvent from the structure. The resulting crystals were tested using SCXRD, but it was found that a single crystal of QDMSO did not give a single crystal of the de-solvated form, therefore the structure of these crystals could not be solved.

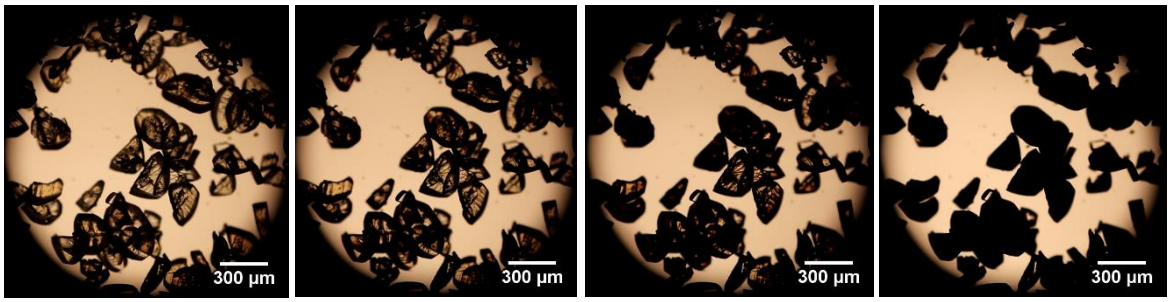

(a) (b) (c) (d)

Figure 7. HSM images of QDMSO at (a) 25 °C, (b) 130 °C, (c) 135 °C, (d) 140 °C

Variable Temperature Powder X-Ray Diffraction (VT-PXRD) analysis. The thermal stability of the two solvates was further analysed using VT-PXRD. XRD patterns of QDH were observed in a temperature range between 25°C and 140°C. This is illustrated in Figure 8 (top). At room temperature the PXRD pattern of QDH exhibited distinct peaks in agreement with the data obtained by Rossi et al. (CSD Refcode: FEFBEX) and with other PXRD patterns for QDH previously reported in literature. [14,24] The PXRD pattern of QDH remained unchanged between 25°C and 70°C, while at 100°C many of the peaks characteristic for QDH (10.70, 16.02, 23.70, 38.54) decreased in intensity indicating the start of a phase transition. The PXRD

pattern stopped changing at 110°C and remained unchanged up to the maximum temperature of 140°C and also upon cooling down to 25°C. This behaviour shows that the resultant quercetin form does not change back to the QDH form after cooling, at least during the time frame of the VT-PXRD experiment. Combining this information with the DSC-TGA analysis, the phase change at 100°C corresponds to the dehydration of QDH. Since no further loss in mass occurred after the first dehydration step, and before decomposition, as indicated by the TGA curve in Figure 6, the PXRD pattern obtained at 110°C should correspond to an anhydrous form of quercetin. It should be noted that the PXRD pattern of this anhydrous polymorph of quercetin does not match with the pattern reported by Vasisht et al. (CSD Refcode: NAFZEC) for the anhydrous structure of quercetin. [18]

The PXRD pattern for QDMSO is illustrated in Figure 8 (bottom). The structure appeared to be stable between 35°C and 100°C. At 120°C a phase change started occurring and a new PXRD pattern was exhibited from 140°C up to 180°C, which remained unchanged when the temperature was reduced to 120°C and further down to 25°C. This phase change corresponds to the loss of the DMSO solvent molecules observed in the DSC-TGA data. The PXRD pattern of the de-solvated QDMSO is almost identical to the PXRD pattern obtained from the dehydration of the QDH, both having common reflections at 2θ values of 12.84, 16.58, 25.87, 26.61, 34.64, 37.21 and 42.80. This suggests that both forms lose the solvent and transform to the same de-solvated polymorph of quercetin.

VT-PXRD and DCS-TGA showed that QDH and QDMSO exhibited different thermal stabilities in their heat-induced de-solvation process: QDH appears to de-solvate at a lower temperature of about 100°C (95°C from DSC-TGA) while the de-solvation for QDMSO begins at a higher temperature of about 120°C (136°C from DSC-TGA). It has been reported in literature that the thermal stability of solvate structures in heat-induced de-solvation is

dependent on the type and strength of intermolecular interactions of solvent molecules with the main compound as well as on crystal packing.[6],[13] Our synthonic modelling work demonstrated that the strongest quercetin-DMSO hydrogen bonds are higher in energy compared to the quercetin-water hydrogen bonds in QDH.

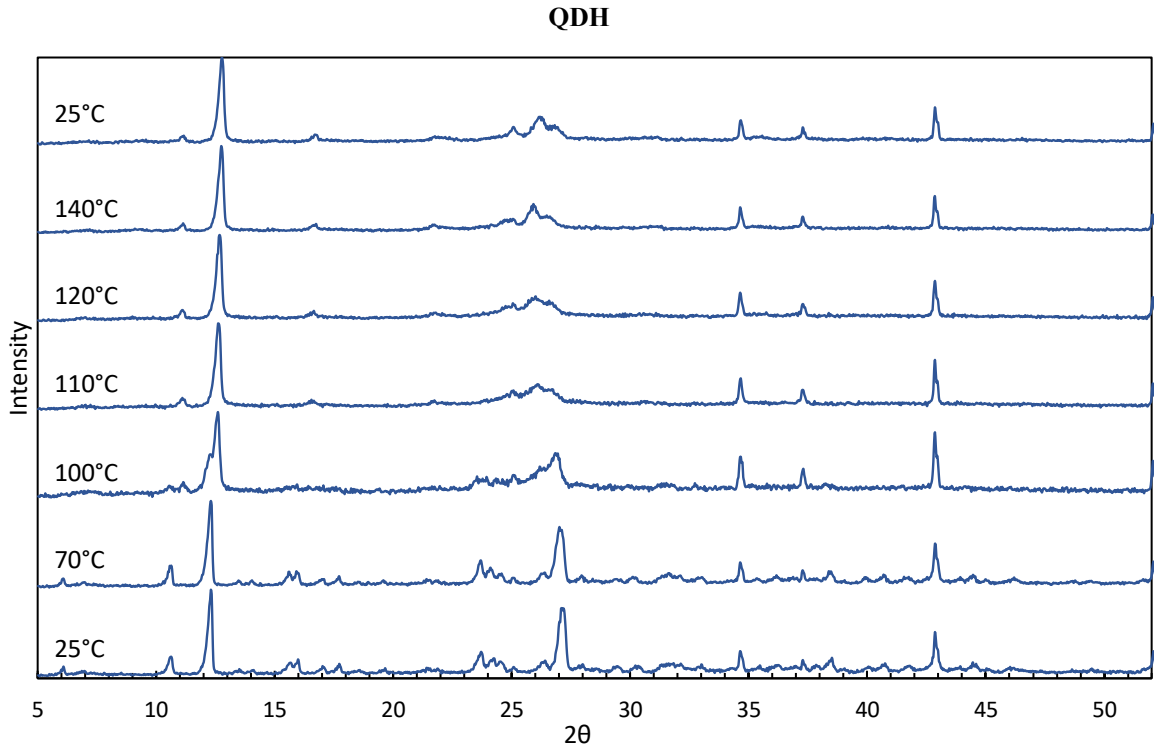

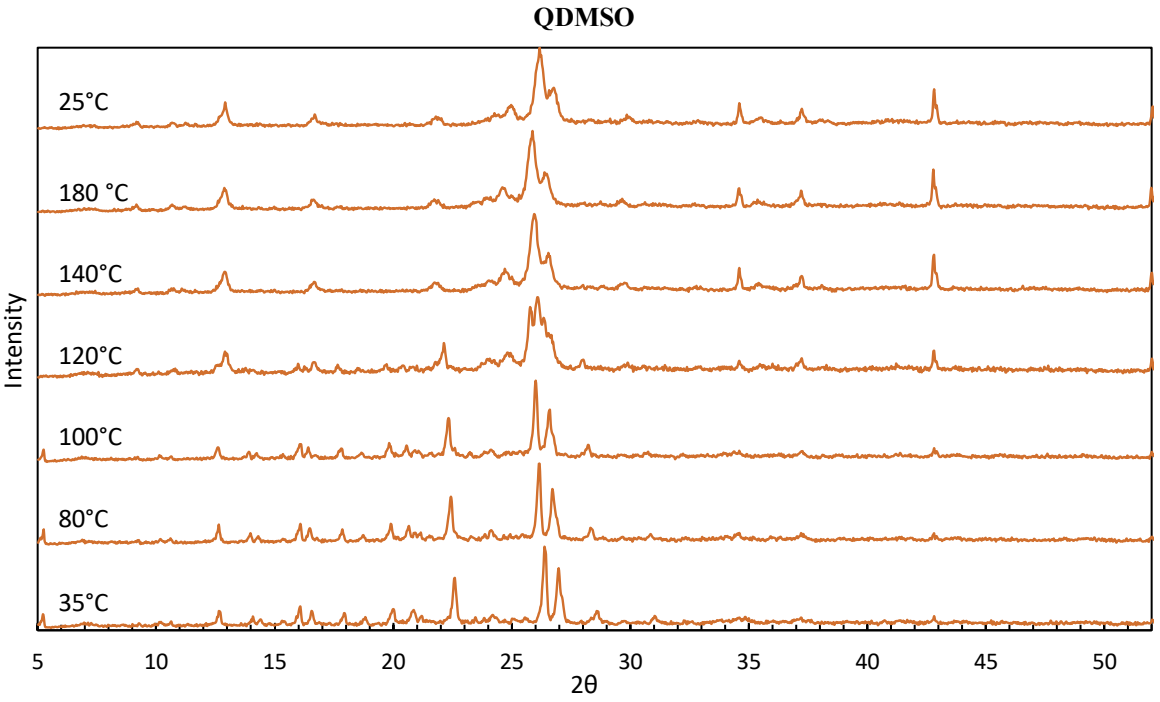

Figure 8. The VT-PXRD patterns for QDH (top) and QDMSO (bottom).

This can explain the greater thermal stability of QDMSO compared to QDH. In fact, more energy is required to break the quercetin-DMSO hydrogen bonds to release the solvent, and this occurs at a higher temperature. The loss of solvent results in a solid-state transformation to a pure quercetin form. It is clear that in both solvates the quercetin-solvent interactions are critical for the stabilization of the crystal lattice. When the solvent molecules are lost during the heat-induced de-solvation, the quercetin molecules rearrange to form new interactions and compensate for the lost quercetin-solvent interactions.

Dynamic Vapour Sorption (DVS) analysis. The moisture-dependent stability of the two solvates was evaluated in a RH range from 0-90%. The mass of QDH appeared to be stable over a wide humidity range from RH=10% to RH=80%, as shown in Figure 9 (top). At RH=90%, both during sorption and desorption, a small increase in the mass of QDH was observed (approximately 2%) which could be a result of adsorption of water moisture on the surface of the QDH crystals. Below RH=10% the mass decreased down to 95% of the initial value. This roughly corresponds to the loss of one water molecule from the lattice per molecule of quercetin (theoretical value of 94.6%) and could indicate a moisture dependent transformation from the dihydrate structure to a monohydrate form. Figure 9 shows that the mass of QDH was still changing at 604 min, when the humidity was changed from RH=0% to RH=10% (this is because the sample reached the maximum allowed time at constant humidity). This behaviour indicates that the loss of water from QDH is slow. During sorption, at RH=10% there was an increase in mass to 98.6% of the initial value, which indicates a potential rehydration of the dehydrated form back to QDH. This behaviour shows that the QDH structure is the stable form for values of RH=10% and above. Once again, the fact that QDH is only unstable at very low RH (below 10%) highlights the importance of the quercetin-water

interactions in the stabilization of the crystal lattice, which were found to contribute to 45.9% of the total lattice energy.

DVS analysis for the QDMSO structure showed that this solvate is stable over a RH range from 0% to 80%, where the sample mass only increased up to 102.2% of the starting mass, most likely because of adsorption of water at the crystal surface. At RH=90% the mass increased significantly to 112% of the initial value. This could be the result of a gain in water molecules and potential transformation of the DMSO solvate into the QHD form. Because of its low volatility the DMSO incorporated in QDMSO will unlikely evaporate during this polymorphic conversion. This explains why the change in mass recorded by DVS corresponds to the water incorporation only.

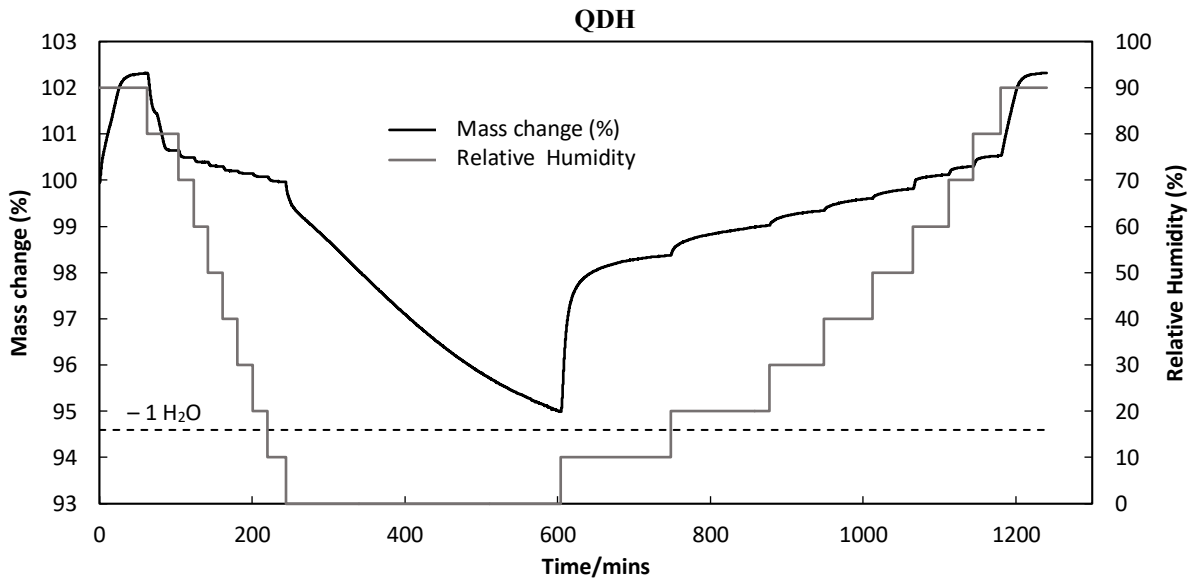

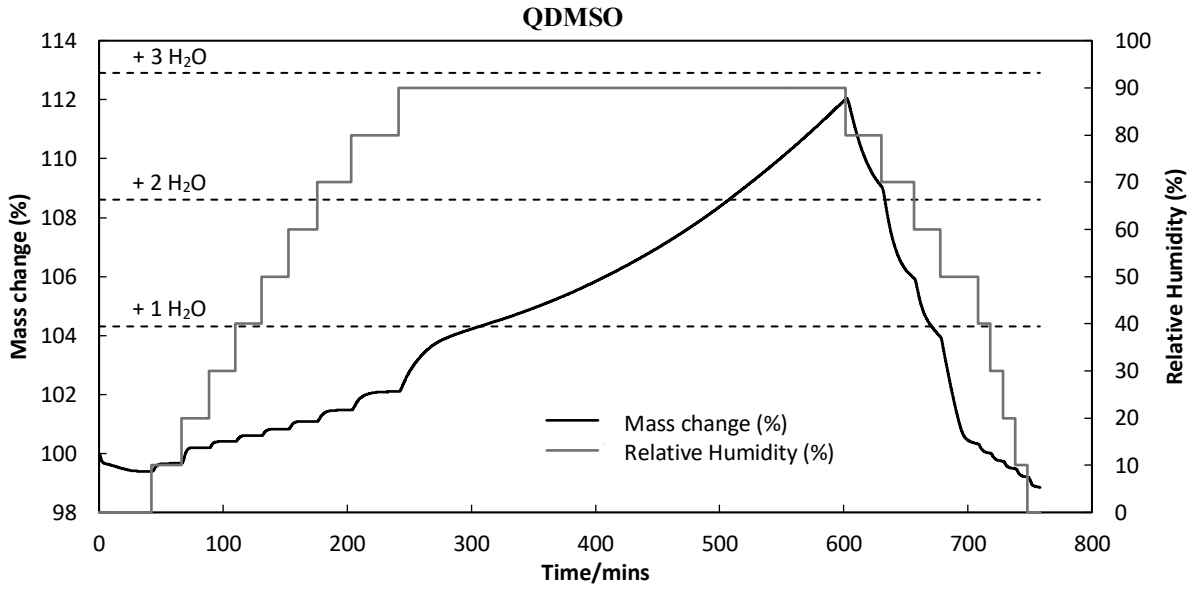

Figure 9. DVS diagrams for QDH (top) and QDMSO (bottom), illustrating the mass change at different relative humidity values. The dotted horizontal lines indicate the theoretical mass change for the loss/gain of water molecules per quercetin molecule in the lattice of each structure.

Figure 9 shows that the mass was still changing at the end of the RH=90% step as the maximum hold time was exceeded, meaning that any transformation to QDH was possibly still ongoing at that time. During desorption the sample lost all the water gained during the sorption step, with the final mass at RH=0% was found to be 98.6% of the initial value, perhaps indicating evaporation of part of the DMSO released from the structure at RH=90. The modelling results for QDMSO showed that the overall energy of the quercetin-DMSO hydrogen bonds was higher than the sum of the energies related to the quercetin-water interactions in QDH. This could explain why QDMSO appeared to be stable over such a wide RH range, and why the quercetin molecules would preferentially form hydrogen bonds with water only above a RH of 80%.

In summary, the DVS results show that, at ambient temperature, QDMSO is stable over a RH range from 0% to 80%, while QDH is stable from 10% to 90% RH, showing slow dehydration at RH=0%.

CONCLUSIONS

Crystallization of quercetin from DMSO-water mixtures resulted in a novel crystal structure of quercetin, a quercetin DMSO-solvate. This form was identified via SCXRD and its physiochemical properties and phase transitions were characterised by VT-PXRD, DSC-TGA, HSM and DVS. The crystal structure packing and bulk intermolecular interactions of QDMSO were studied and compared to other quercetin structures (quercetin anhydrous, monohydrate and dihydrate) and experimental solid-state characterisation was performed for QDMSO and QDH.

It was found that quercetin molecules in QDMSO assume a less planar conformation compared to QDH and QMH, which results in slightly higher intermolecular distances between the interacting molecules, and lower unit cell density. This can be attributed to the larger size of the DMSO molecules compared to water. Molecular modelling calculations showed that the contribution of hydrogen bonds and dipole-dipole interactions to the total lattice energy was much higher for QDMSO compared to all other quercetin structures. Also, the stronger quercetin-DMSO hydrogen bonds can explain the improved thermal stability of QDMSO compared to that of QDH. It was further demonstrated that both QDMSO and QDH transform to the same anhydrous form after heat-induced de-solvation, which was found to generate molecular packing rearrangements in the lattice. DVS showed that the QDH structure was stable above RH=10% while it exhibited dehydration below that. QDMSO was stable from

RH=0% to RH=80%, with a possible transformation to QDH above RH=80%. Both the kinetics of dehydration of QDH and the transformation of QDMSO were found to be slow.

In summary, the novel solvated structure of quercetin, QDMSO, exhibits superior thermal stability compared to that of QDH which is the commercial form of quercetin.

The work demonstrates how synthonic modelling can be used to explain many of the physiochemical properties of solvated quercetin crystals via finding strong correlations between experimental findings and type/strength of intermolecular interactions. This multiangle characterization method, which couples computational and experimental techniques can be applied for other systems, and observations regarding the type and strength of interactions and packing can be extended to other solvated crystalline structures. The presented work can also assist in the ongoing effort to design and predict the behaviour of crystallization processes. In fact, the synthonic modelling methodology proposed here can be used during solid form screening of crystalline products such as pharmaceuticals or agrochemicals, to guide the design of crystallization conditions, such as the choice of solvent, and to infer the physiochemical properties of the generated crystal forms without the need of a large number of experiments. This is particularly useful when little amount of crystallizing material is available, for example in early drug development stages, and it can result in faster product and process development.

ACKNOWLEDGEMENTS

The authors acknowledge the Bragg Centre for Materials Research at the University of Leeds for the technical support in running experiments and analysing data of X-ray diffraction and electron microscopy facilities. Dr Simone would like to acknowledge the Royal Academy of Engineering (grant n IF\192031) for financial support.

SUPPORTING INFORMATION

The supporting information associated to this work contains the crystallographic data, structure refinement details and hydrogen bonding parameters for the QDMSO crystal structure. A table summarizing the characteristics of all solid forms of quercetin mentioned in the paper is also presented. Finally, quantitative details of the DSC-TGA thermal analysis for QDH and QDMSO are reported. This material is available free of charge via the internet at http://pubs.acs.org.

REFERENCES

(1) Healy, A. M.; Worku, Z. A.; Kumar, D.; Madi, A. M. Pharmaceutical Solvates, Hydrates and Amorphous Forms: A Special Emphasis on Cocrystals. *Adv. Drug Deliv. Rev.* **2017**, *117*, 25–46. https://doi.org/10.1016/j.addr.2017.03.002.

(2) Threlfall, T. L. Analysis of Organic Polymorphs. A Review. *Analyst* **1995**, *120*, 2435–2460. https://doi.org/10.1039/AN9952002435.

(3) Tilbury, C. J.; Chen, J.; Mattei, A.; Chen, S.; Sheikh, A. Y. Combining Theoretical and Data-Driven Approaches To Predict Drug Substance Hydrate Formation. **2018**. https://doi.org/10.1021/acs.cgd.7b00517.

(4) Vippagunta, S. R.; Brittain, H. G.; Grant, D. J. W. Crystalline Solids. **2001**, *48*, 3–26.

(5) Griesser, U. J. The Importance of Solvates. *Polymorphism*. May 22, 2006. https://doi.org/doi:10.1002/3527607889.ch8.

(6) Zhu, B.; Zhang, Q.; Ren, G.; Mei, X. Solid-State Characterization and Insight into Transformations and Stability of Apatinib Mesylate Solvates. *Cryst. Growth Des.* **2017**, *17*, 5994–6005. https://doi.org/10.1021/acs.cgd.7b01123.

(7) Reutzel-Edens, S. M.; Bush, J. K.; Magee, P. A.; Stephenson, G. A.; Byrn, S. R. Anhydrates and Hydrates of Olanzapine: Crystallization, Solid-State Characterization, and Structural Relationships. *Cryst. Growth Des.* **2003**, *3*, 897–907. https://doi.org/10.1021/cg034055z.

(8) Groenendaal, J. W.; Antonius Maria Leenderts, E. J.; VanvDer Does, T. AMOXCILLIN TRHYDRATE. US 2006/0172987 A1, 2006.

(9) Ahire, V.; Sasane, S.; Deshmukh, A.; Kumbhar, K.; Bhatnagar, A.; Verma, D.; Vyas, R.; Singh, G. P.; Bishe, N. PROCESS FOR PREPARATION OF DARUNAVIR AND DARUNAVIR ETHANOLATE OF FINE PARTICLE SIZE. US 9,062,065 B2, 2015.

(10) Li, J.; Tilbury, C. J.; Kim, S. H.; Doherty, M. F. A Design Aid for Crystal Growth Engineering. *Prog. Mater. Sci.* **2016**, *82*, 1–38. https://doi.org/10.1016/j.pmatsci.2016.03.003.

(11) Sung, H.; Fan, Y.; Yeh, K.; Chen, Y.; Chen, L. Colloids and Surfaces B : Biointerfaces A New Hydrate Form of Diflunisal Precipitated from a Microemulsion System. **2013**, *109*, 68–73.

(12) Bauer, J.; Spanton, S.; Henry, R.; Quick, J.; Dziki, W.; Porter, W.; Morris, J. Ritonavir: An Extraordinary Example of Conformational Polymorphism. *Pharm. Res.* **2001**, *18*, 859–866. https://doi.org/10.1023/a:1011052932607.

(13) Zhu, B.; Fang, X.; Zhang, Q.; Mei, X.; Ren, G. Study of Crystal Structures, Properties, and Form Transformations among a Polymorph, Hydrates, and Solvates of Apatinib. *Cryst. Growth Des.* **2019**, *19*, 3060–3069. https://doi.org/10.1021/acs.cgd.9b00397.

(14) Rossi, M.; Rickles, L. F.; Halpin, W. A. The Crystal and Molecular Structure of Quercetin: A Biologically Active and Naturally Occurring Flavonoid. *Bioorg. Chem.* **1986**, *14*, 55–69. https://doi.org/10.1016/0045-2068(86)90018-0.

(15) Srinivas, K.; King, J. W.; Howard, L. R.; Monrad, J. K. Solubility and Solution

Thermodynamic Properties of Quercetin and Quercetin Dihydrate in Subcritical Water. *J. Food Eng.* **2010**, *100*, 208–218. https://doi.org/10.1016/j.jfoodeng.2010.04.001.

(16) Luo, Z.; Murray, B. S.; Yuso, A.; Morgan, M. R. a; Povey, M. J. W.; Day, A. J. Particle-Stabilizing Effects of Flavonoids at the Oil - Water Interface. *J. Agric. ...* **2011**, *59*, 2636–2645.

(17) Ay, M.; Charli, A.; Jin, H.; Anantharam, V.; Kanthasamy, A.; Kanthasamy, A. G. Quercetin. *Nutraceuticals* **2016**, 447–452. https://doi.org/10.1016/B978-0-12-802147-7.00032-2.

(18) Vasisht, K.; Chadha, K.; Karan, M.; Bhalla, Y.; Jena, A. K.; Chadha, R. Enhancing Biopharmaceutical Parameters of Bioflavonoid Quercetin by Cocrystallization. *CrystEngComm* **2016**, *18*, 1403–1415. https://doi.org/10.1039/C5CE01899D.

(19) Domagała, S.; Munshi, P.; Ahmed, M.; Guillot, B.; Jelsch, C. Structural Analysis and Multipole Modelling of Quercetin Monohydrate - A Quantitative and Comparative Study. *Acta Crystallogr. Sect. B Struct. Sci.* **2011**, *67*, 63–78. https://doi.org/10.1107/S0108768110041996.

(20) Nifant'ev, E. E.; Koroteev, M. P.; Kaziev, G. Z.; Uminskii, A. A.; Grachev, A. A.; Men'shov, V. M.; Tsvetkov, Y. E.; Nifant'ev, N. E.; Bel'skii, V. K.; Stash, A. I. On the Problem of Identification of the Dihydroquercetin Flavonoid. *Russ. J. Gen. Chem.* **2006**, *76*, 161–163. https://doi.org/10.1134/S1070363206010324.

(21) Jin, G. Z.; Yamagata, Y.; Tomita, K. Structure of Quercetin Dihydrate. *Acta Crystallogr. Sect. C Cryst. Struct. Commun.* **1990**, *46*, 310–313. https://doi.org/10.1107/S0108270189006682.

(22) Klitou, P.; Rosbottom, I.; Simone, E. Synthonic Modeling of Quercetin and Its Hydrates: Explaining Crystallization Behavior in Terms of Molecular Conformation and Crystal Packing. *Cryst. Growth Des.* **2019**, *19*, 4774–4783.

https://doi.org/10.1021/acs.cgd.9b00650.

(23) Olejniczak, S.; Potrzebowski, M. J. Solid State NMR Studies and Density Functional Theory (DFT) Calculations of Conformers of Quercetin†. **2004**, 2315–2322.

(24) Borghetti, G. S.; Carini, J. P.; Honorato, S. B.; Ayala, A. P.; Moreira, J. C. F.; Bassani, V. L. Thermochimica Acta Physicochemical Properties and Thermal Stability of Quercetin Hydrates in the Solid State. *Thermochim. Acta* **2012**, *539*, 109–114. https://doi.org/10.1016/j.tca.2012.04.015.

(25) Spiteri, L.; Baisch, U.; Vella-Zarb, L. Correlations and Statistical Analysis of Solvent Molecule Hydrogen Bonding – a Case Study of Dimethyl Sulfoxide (DMSO). *CrystEngComm* **2018**, *20*, 1291–1303. https://doi.org/10.1039/C7CE02206A.

(26) Desiraju, G. R. Supramolecular Synthons in Crystal Engineering—A New Organic Synthesis. *Angew. Chemie Int. Ed. English* **1995**, *34*, 2311–2327. https://doi.org/10.1002/anie.199523111.

(27) Desiraju, G. R. Crystal Engineering: Structure, Property and beyond. *IUCrJ* **2017**, *4*, 710–711. https://doi.org/10.1107/S2052252517014853.

(28) Sheldrick, G. M. {\it SHELXT} {--} Integrated Space-Group and Crystal-Structure Determination. *Acta Crystallogr. Sect. A* **2015**, *71*, 3–8. https://doi.org/10.1107/S2053273314026370.

(29) Sheldrick, G. M. Crystal Structure Refinement with {\it SHELXL}. *Acta Crystallogr. Sect. C* **2015**, *71*, 3–8. https://doi.org/10.1107/S2053229614024218.

(30) AS, I. Discovery Studio Modeling Environment, Release 7.0 [Software Program]. Accelrys Software Inc.: San Diego 2013.

(31) Clydesdale, G.; Roberts, K. J.; Docherty, R. HABIT95 — a Program for Predicting the Morphology of Molecular Crystals as a Function of the Growth Environment. *J. Cryst. Growth* **1996**, *166*, 78–83. https://doi.org/10.1016/0022-0248(96)00056-5.

(32) Van de Streek, J.; Motherwell, S. New Software for Searching the Cambridge Structural Database for Solvated and Unsolvated Crystal Structures Applied to Hydrates. *CrystEngComm* **2007**, *9*, 55–64. https://doi.org/10.1039/B613332K.

(33) Stewart, J. J. P. M. MOPAC for Solid-State Physics. Quant. Chem. Prog. Exchange 1985, p 62.63.

(34) Pickering, J.; Hammond, R. B.; Ramachandran, V.; Soufian, M.; Roberts, K. J. Synthonic Engineering Modelling Tools for Product and Process Design. In *Engineering Crystallography: From Molecule to Crystal to Functional Form*; Roberts, K. J., Docherty, R., Tamura, R., Eds.; Springer Netherlands: Dordrecht, 2017; pp 155–176. https://doi.org/10.1007/978-94-024-1117-1_10.

(35) Rosbottom, I.; Roberts, K. J.; Docherty, R. The Solid State, Surface and Morphological Properties of *P* -Aminobenzoic Acid in Terms of the Strength and Directionality of Its Intermolecular Synthons. *CrystEngComm* **2015**, *17*, 5768–5788. https://doi.org/10.1039/C5CE00302D.

(36) Mayo, S. L.; Olafson, B. D.; Goddard, W. A. DREIDING: A Generic Force Field for Molecular Simulations. *J. Phys. Chem.* **1990**, *94*, 8897–8909. https://doi.org/10.1021/j100389a010.

(37) Parker, L. L.; Houk, A. R.; Jensen, J. H. Cooperative Hydrogen Bonding Effects Are Key Determinants of Backbone Amide Proton Chemical Shifts in Proteins. *J. Am. Chem. Soc.* **2006**, *128*, 9863–9872. https://doi.org/10.1021/ja0617901.

(38) Walshe, N.; Crushell, M.; Karpinska, J.; Erxleben, A.; McArdle, P. Anisotropic Crystal Growth in Flat and Nonflat Systems: The Important Influence of van Der Waals Contact Molecular Stacking on Crystal Growth and Dissolution. *Cryst. Growth Des.* **2015**, *15*, 3235–3248. https://doi.org/10.1021/acs.cgd.5b00348.

(39) Cruz-Cabeza, A. J.; Davey, R. J.; Oswald, I. D. H.; Ward, M. R.; Sugden, I. J.

Polymorphism in P-Aminobenzoic Acid. *CrystEngComm* **2019**, *21*, 2034–2042. https://doi.org/10.1039/C8CE01890A.

(40) Costa, E. M.; Filho, J. M. B.; do Nascimento, T. G.; Macêdo, R. O. Thermal Characterization of the Quercetin and Rutin Flavonoids. *Thermochim. Acta* **2002**, *392–393*, 79–84. https://doi.org/https://doi.org/10.1016/S0040-6031(02)00087-4.

FOR TABLE OF CONTENTS USE ONLY

Solid-State Characterization and Role of Solvent Molecules on the Crystal Structure, Packing and Physiochemical Properties of Different Quercetin Solvates

*Panayiotis Klitou1, Christopher M. Pask2, Larisa Onoufriadi3, Ian Rosbottom4, Elena Simone*1*

1School of Food Science and Nutrition, Food Colloids and Bioprocessing Group, University of Leeds, Leeds, UK

2 School of Chemistry, University of Leeds, Leeds, UK

3 School of Chemical and Process Engineering, University of Leeds, Leeds, UK

4 Department of Chemical Engineering, Imperial College London, South Kensington Campus, London, UK

*Corresponding author: e.simone@leeds.ac.uk

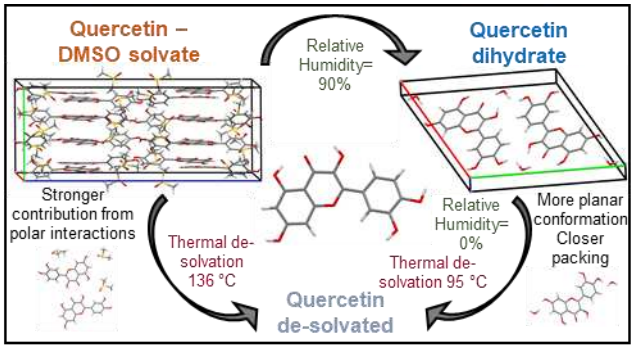

Synopsis: A novel dimethyl sulfoxide solvate structure of quercetin was characterized experimentally and via synthonic modelling. Results were compared to those of other known quercetin structures to elucidate the role of solvent molecules on the molecular packing and intermolecular interactions of each of these crystal forms.